УДК 620.187.620.1

O.D. Vasylyev[1], A.L. Smirnova[2], M.M. Brychevskyi[1], I.M. Brodnikovskyi[1], S.O. Firstov[1], V.G. Vereschak[3], G.Ya. Akimov[4], Yu.O. Komysa[4], J.T.S. Irvine[5], C.-D. Savaniu[5], V.A. Sadykov[6], I. Kosacki[7]

[1] I.M. Frantcevych Institute for Problems of Materials Science
Krzhyzhanovs'ky Str., 3, 03680, Kyiv, Ukraine

[2] Environmental Earth Science, Eastern Connecticut State University, Science Building
Windham Rd., 83, Willimantic, CT, 06226, USA

[3] Ukrainian State Chemical and Technological University
Gagarin Ave., 8, 49005, Dnipropetrovs'k, Ukraine

[4] O.O. Galkin Donets'k Institute for Physics and Engineering
Rosa Luxemburg Str., 72, 83114, Donets'k, Ukraine

[5] School of Chemistry, University of St. Andrews
Fife KY16 9ST, Scotland, UK

[6] Boreskov Institute of Catalysis
Lavrentiev Academician Ave., 5, Novosibirsk, 630090, RF

[7] Westhollow Technology Center, Shell Co
3333, Highway 6 South, Houston, TX 77082-3101, USA

STRUCTURAL, MECHANICAL, AND ELECTROCHEMICAL PROPERTIES OF CERIA DOPED SCANDIA STABILIZED ZIRCONIA

Key words: *nanopowders, scandia stabilized zirconia, 1Ce10ScSZ, solid electrolyte, fracture toughness, biaxial strength, solid oxide fuel cells*

The properties of Ceria doped Scandia Stabilized Zirconia (1Ce10ScSZ) nano-powder produced in Ukraine (Ukr, VMMP) are compared to the properties of commercial ones produced by Daiichi Kigenso Kagaku Kogyo (DKKK, Japan) and Praxair (USA). In comparison to DKKK and Praxair, the Ukr nano-powder demonstrated the smallest size of the particles ranging from 20 to 50 nm. The bending strength of the isostatically pressed samples made of Ukr powder was 100–120 MPa similar to that of Praxair. The bending strength of DKKK was lower (50–100 MPa) depending on the isostatic pressure. The biaxial strength of uniaxially pressed samples was the highest for DKKK (375 MPa) decreasing to 250 MPa for Ukr and 220 MPa for Praxair. Among three tested samples, the highest electric conductivity measured at 700°C was found for Ukr electrolyte.

Introduction

Scandia stabilized zirconia (ScSZ) is known as an attractive alternative to the conventional yttria stabilized zirconia electrolyte (YSZ) and is commonly used for sensors [1], solid oxide fuel cells (SOFC) [2], and solid state electrolyzes [3] since it exhibits the highest ionic conductivity among zirconia-based solid solutions [4, 5]. The maximum conductivity was observed for the electrolytes with 10% Sc_2O_3 in ScSZ [6]. However, it was found that in ScSZ ceramics at less than 10 mol.% Sc_2O_3 a transition from cubic into rhombohedral phase takes place which is accompanied by significant

degradation of electrical conductivity. In order to suppress the phase transformation, ScSZ is usually doped with small amounts of ceria or alumina [7, 8].

This work presents the results on morphology, sintering properties, mechanical behavior, and electric conductivity of the zirconia stabilized with 10% Sc_2O_3 and 1% CeO_2 (1Ce10ScSZ) nano-powders synthesized from abundant Ukrainian Zirconia natural resources. The results are discussed in comparison to the data obtained for commercially available powders from DKKK and Praxair.

Experimental

1Ce10ScSZ nano-powder was produced at Vil'nohirs'k Mining and Metallurgical Plant (VMMP), Ukraine, according to the co-precipitation technique developed earlier on laboratory scale [9]. Briefly, $ZrOCl_2 \cdot 8H_2O$ and Sc_2O_3 commercially produced at VMMP from the natural Ukrainian resource were used for the synthesis of 1Ce10ScSZ. The initial solution was prepared by dissolving $ZrOCl_2 \cdot 8H_2O$ in distilled water at 60 °C with appropriate amount of Sc_2O_3 added and dissolved afterward under stirring conditions. After that, 1 mol.% of Ce^{4+} in the form of $CeCl_4$ was added and the resulting solution was left for 24 h at room temperature. The process of co-precipitation was performed at pH = 9.5 by adjusting the solution basicity using NH_4OH. The precipitate was washed with distilled water to remove Cl^- and NH_4^+ ions. In order to avoid formation of the aggregates, the formed hydroxides were dried by azeotropic distillation with butyl alcohol [10] followed by sintering of the xerogels at 700–850 °C in air.

The crystal structure, the agglomerate size, and the surface area of the 1Ce10ScSZ powders were studied using XRD (DRON, «Burevestnik», RF), laser granulometry [11] and BET respectively. The morphology of the powders was analyzed using TEM (JEM 100CXII, JEOL, Japan); and SEM (Superprobe 733, JEOL).

For mechanical testing, the rectangular bars of 4·4·40 mm^3 were isostatically cold pressed in the range of 20–80 MPa at room temperature (CIP), and sintered at 1550 °C for 1.5 h. The bars were polished with diamond pastes for evaluation of a three points bending strength. The fracture toughness was measured with the samples notched with a 150 μm thick diamond blade. The preliminary biaxial strength tests for the evaluation of the optimal sintering temperature were performed with the unpolished pellets (15 mm in diameter and 2 mm thick) that were uniaxially pressed [12] at 20 MPa and sintered at 1250–1550 °C for 1.5 h with 100 °C/h heating rate.

The information regarding the surface/bulk compositions of the powders was obtained using Secondary Ions Mass Spectrometry (SIMS) with MC-7201. For SIMS studies, the powders were rubbed into a high-purity indium substrate. An argon ion beam with energy of 3 KeV and current density of 5 μA/cm^2 was used for sputtering. The thickness of the layers removed with argon bombardment was calculated from the sputtering time. The electrical properties of the ceramic samples was performed using Solartron 1260 analyzer in air in the temperature range of 250–850 °C. Platinum ink (Engelhard) was used for the electrodes coating on each side of the pellets, followed by firing at 900 °C for 1 h.

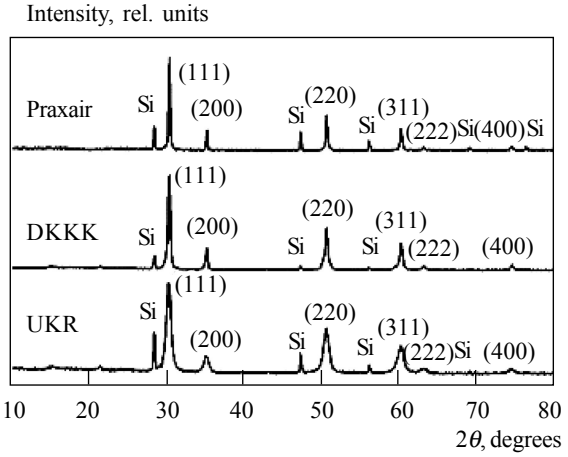

Fig. 1. X-ray diffraction spectra of the 1Ce10ScSZ Ukr, DKKK, and Praxair powders. Si lines are the reference marks

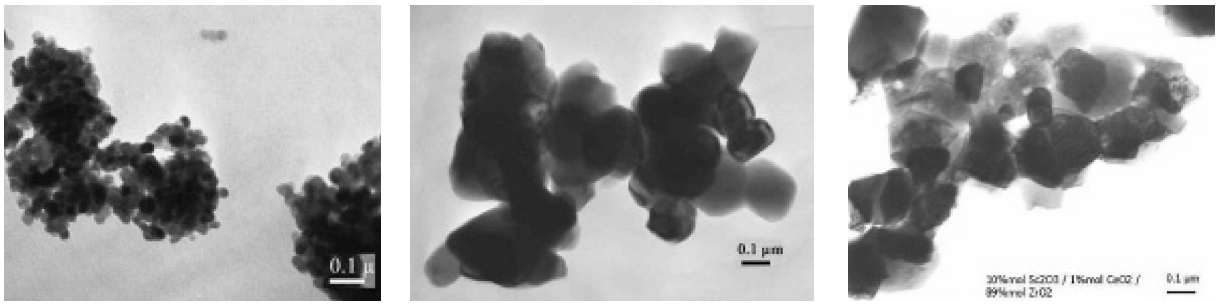

a *b* *c*

Fig. 2. TEM images of the 1Ce10ScSZ powders: (*a*) Ukr, (*b*) DKKK, and (*c*) Praxair

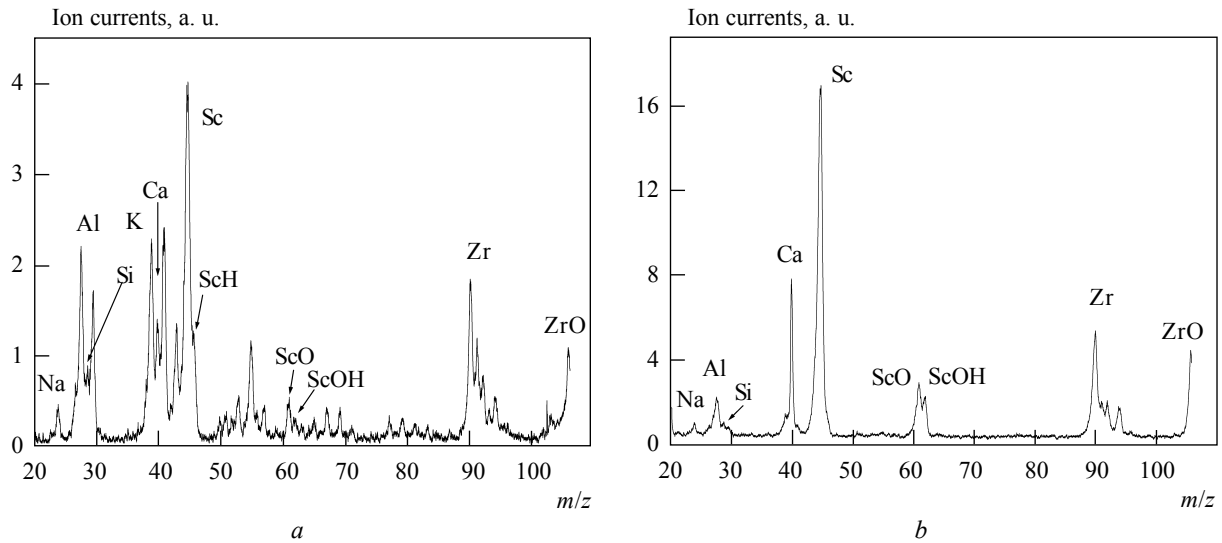

a *b*

Fig 3. SIMS mass-spectra of the 1Ce10ScSZ-Ukr powder: (*a*) surface layer and (*b*) bulk

Results and their discussion

Morphology, structure, and composition

The X-ray diffraction patterns revealed the cubic structure for all three 1Ce10ScSZ powders (Fig.1). The observed broadening of the diffraction peaks (Ukr > DKKK > Praxair) was in correlation with the changes of the specific surface area of the samples. The surface area was the highest for 1Ce10ScSZ-Ukr (48.28 m^2/g) and the lowest for 1Ce10ScSZ-Praxair (4.98 m^2/g). This was also confirmed by the TEM images of the powders (Fig. 2). It can be seen that 1Ce10ScSZ-Ukr has the smallest particle size in the range of 20–50 nm while the corresponding values for 1Ce10ScSZ-DKKK and 1Ce10ScSZ-Praxair were significantly higher as reflected in Table.

Table. Geometrical properties of zirconia powders studied

Powder produced by	Particles, nm	Agglomerates, μm	Specific surface, m^2/g
Ukr	20–50	2.4	48.28
DKKK	100–200	0.5–1.0*	11.61
Praxair	100–300	18.1	4.98

*data obtained by TEM

It was found that the Praxair rigid agglomerates impede sintering process, while DKKK soft agglomerate structure favors sintering and densification. The sintering properties of the

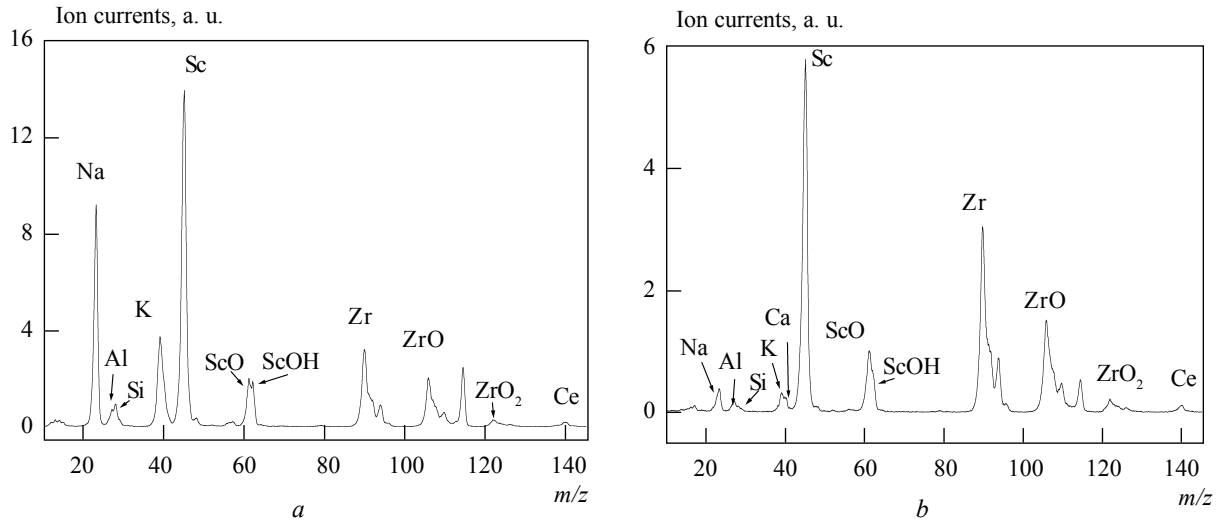

Fig. 4. SIMS mass-spectra of the 1Ce10ScSZ-Praxair powder: (*a*) surface layer and (*b*) bulk

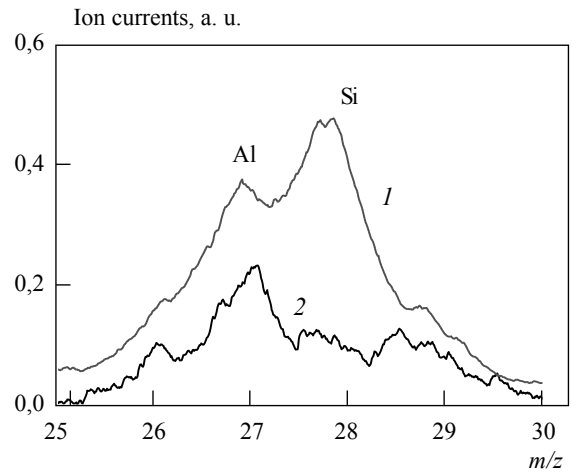

Fig. 5. Relative content of Si and Al in the surface layers of the 1Ce10ScSZ powders: (*1*) Praxair and (*2*) DKKK

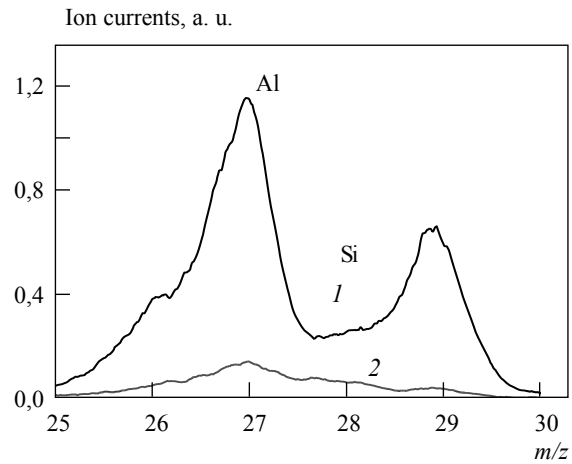

Fig. 6. Relative content of Al and Si in 1Ce10ScSZ-DKKK powder: (*1*) bulk and (*2*) surface layer

synthesized 1Ce10ScSZ-Ukr nano-powder were in-between Praxair and DKKK.

The analysis of the surface and bulk chemical composition of the 1Ce10ScSZ-Ukr and commercial powders demonstrated a presence of oxide impurities such as Al_2O_3, MgO, TiO_2, and SiO_2. It was confirmed that 1Ce10ScSZ-DKKK powder contains almost negligible ($<10^{-3}$ wt.%) amounts of impurities. The amount of impurities in 1Ce10ScSZ-Ukr and Praxair powders was much higher. Such as 1Ce10ScSZ-Ukr contained 0.025 wt.% Al_2O_3 and 0.02 wt.% MgO, on the other hand in Praxair powder 0.14 wt.% TiO_2 was detected. Both 1Ce10ScSZ-Ukr and Praxair contained about 0.05 wt.% SiO_2 and negligible traces of other elements such as K, Na, Ca, and Fe.

SIMS data for 1Ce10ScSZ-Ukr and Praxair powders (Fig. 3 and 4) indicate that the admixtures are present in the surface and in the bulk with a clear trend for segregation on the surface. For example, the accumulation of Al and Si on the surface of Praxair powder is higher than in the bulk. Regarding Sc as the second main component of the 1Ce10ScSZ solid solution, we can conclude that

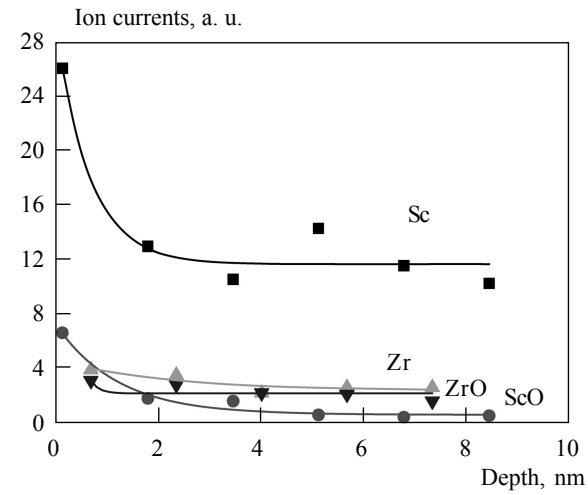

Fig. 7. Changes of the ion currents with sputtering depth for DKKK 1Ce10ScSZ sample

the surface of 1Ce10ScSZ-Ukr is depleted with Sc (Fig. 3) while in Praxair powder the situation is opposite: the intensity of Sc-peak from the surface is higher than from the bulk (Fig. 4). It can be seen that in the case of 1Ce10ScSZ-Praxair, Si is detected on the surface rather than in the bulk that can decrease the ionic conductivity.

The relative content of Si and Al in the commercially available 1Ce10ScSZ powders is presented in Fig. 5 and 6. It can be seen that in comparison to 1Ce10ScSZ-Praxair, the DKKK powder contains half Al and practically no Si. In the Praxair sample the Si content, as mentioned above, is much higher in the surface layer than in the bulk. In Fig. 7 some enrichment of the surface layer by Sc in DKKK sample can be observed, which may be due to the different synthesis procedures.

Mechanical behavior

The biaxial bending strength of uniaxially pressed ceramics made of three 10Sc1CeSZ powders vs. sintering temperature is presented in Fig. 8*a*. The biaxial strength of 1Ce10ScSZ-Ukr reached the maximum of 240 MPa after sintering at 1500 °C. However, at lower sintering temperatures it was the lowest among the three tested samples with the cleavage fracture mechanism and high porosity (Fig. 9*a*). 1Ce10ScSZ-Ukr ceramics fail with cleavage at all the temperatures of sintering above 1350 °C. It was observed that the particles begin to consolidate at temperature not less 1350 °C. At 1450 °C all particles are joined with each other with no visible densification. At 1550 °C the well-joined but relatively porous structure was formed. It is important that the grains fail with cleavage mechanism demonstrating strong adhesion between particles and agglomerates.

The uniaxially pressed 1Ce10ScSZ-Praxair samples sintered at different temperatures demonstrated a change in biaxial strength and fracture mechanism, for example, an intergranular fracture at 1350 °C, cleavage at 1450 °C, and intergranular fracture at 1550 °C. The biaxial strength of 1Ce10ScSZ-Praxair sintered at 1450 °C reached

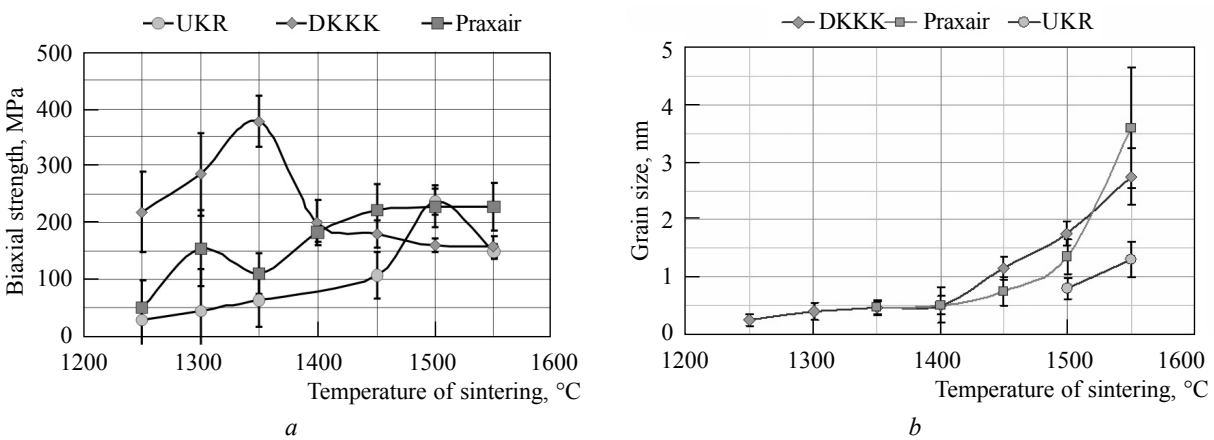

Fig. 8. The properties of the uniaxially pressed 1Ce10ScSZ DKKK, Ukr, and Praxair powders vs. sintering temperature: *a*) biaxial bending strength and *b*) grain size

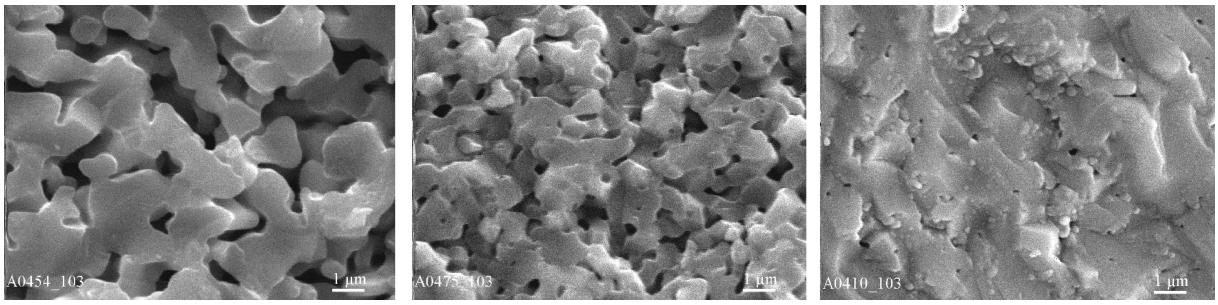

a *b* *c*

Fig. 9. SEM images of the fracture surfaces of the uniaxially pressed 10Sc1CeSZ powders revealing the cleavage mechanism: (*a*) Ukr sintered at 1550 °C; (*b*) Praxair sintered at 1450 °C; and (*c*) DKKK sintered at 1350 °C

its maximum at 220 MPa and fail with cleavage (Fig. 9*b*). Uniaxially pressed 1Ce10ScSZ-DKKK sintered in the temperature range of 1350–1400 °C had the maximum biaxial strength about 375 MPa (Fig. 8*a*) among all three tested samples and fail with cleavage fracture mechanism (Fig. 9*c*). Increase in sintering temperature resulted in significant decrease of the strength down to 180–150 MPa (Fig. 8*a*).

The study of fracture surfaces of 1Ce10ScSZ-DKKK ceramics showed that it started to sinter at rather low temperatures (about 1250 °C) reaching the highest density at 1350 °C (Fig. 9*c*). However, it can be seen that the process of grain sintering is not completed at this temperature that is confirmed by micro-cracking and similarity with some intergranular fracture typical for fine grain ceramics. This sub-grain structure is the possible reason for relatively high biaxial strength of DKKK ceramics sintered in the temperature range of 1250–1350 °C. After sintering at 1450 °C, the strength dramatically decreased to 150–180 MPa level (Fig. 8*a*) with the grain size reaching 5–10 mm at 1550 °C (Fig. 8*b*). The high adhesion between grains was confirmed by the cleavage fracture mechanism.

In comparison to 1Ce10ScSZ-DKKK, the 1Ce10ScSZ-Ukr and 1Ce10ScSZ-Praxair samples did not show any visible changes while applying high isostatic pressure at room temperature. However, 1Ce10ScSZ-DKKK resulted in significant decrease of the bend strength (Fig. 10). It can be seen that the pressure has a negative effect on the strength of 1Ce10ScSZ-DKKK that dropped from 150 MPa to 40 MPa. The deviation of the bend strength values decreased significantly from ±150 MPa at 20 MPa to ±10–20 MPa at 80 MPa of isostatic pressure. This tendency has not been observed for 1Ce10ScSZ-Praxair and 1Ce10ScSZ-Ukr samples where the deviation of the bend strength reached 150–170 MPa in the whole range of the applied pressures.

The insets of the SEM images of 1Ce10ScSZ-DKKK fracture (Fig. 10*a, b*) show that the isostatic pressure influences the fracture mechanism of the samples sintered at 1550 °C promoting the grain and pore growth. The grain size was increasing with pressure from 3–7 mm to 7–25 mm while the density of DKKK ceramics decreased from 5.59 to 5.48 g/cm^3 for the isostatic pressure changed from 20 to 80 MPa respectively [9]. The size and morphology of pores, mainly intergranular, were also changing. The pores in 1Ce10ScSZ-DKKK made at 20 MPa (Fig. 10*a*) were mainly spherical with 0.5–2 μm in diameter, however, they became significantly larger at 80 MPa (Fig. 10b). As a result of the grains and the pore growth, the degradation of the 1Ce10ScSZ-DKKK bending strength took place, which dropped below 50 MPa at 80 MPa pressures (Fig. 10a). The fracture toughness of the isostatically pressed 1Ce10ScSZ-DKKK samples was 0.7–1.2 MPa·m$^{1/2}$.

The 1Ce10ScSZ-Ukr samples at isostatic pressures of 20–80 MPa did not indicate any influence on the three point bend strength and the corresponding values approached 200–220 MPa. The density of 1Ce10ScSZ-Ukr slightly increased with pressure, though the changes in structure were not so obvious (Fig. 11). The fracture mechanism of 1Ce10ScSZ-Ukr ceramics is considered as trans-granular

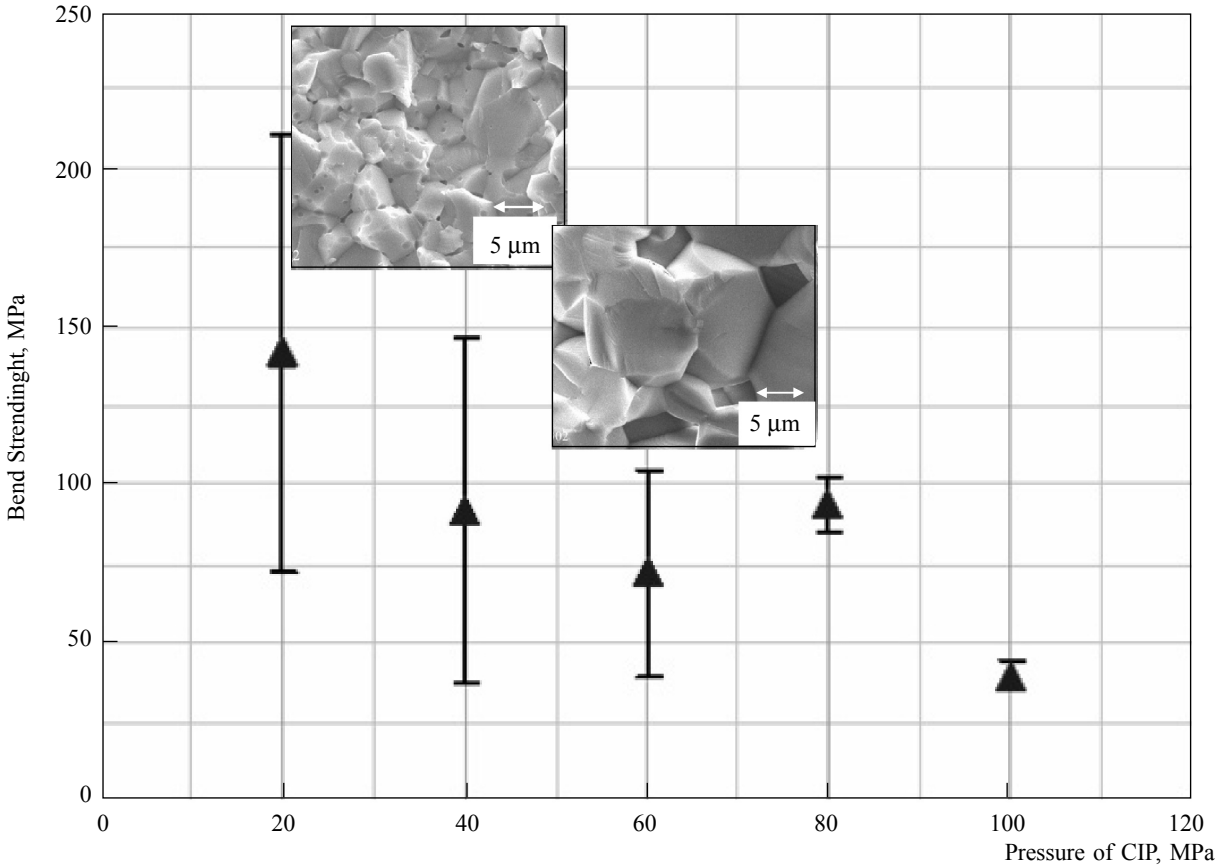

Fig. 10. Three-point bend strength of the isostatically pressed and sintered at 1550 °C 1Ce10ScSZ-DKKK powders vs. pressure. The insets show the SEM images of the samples pressed at (*a*) 20 MPa and (*b*) 80 MPa

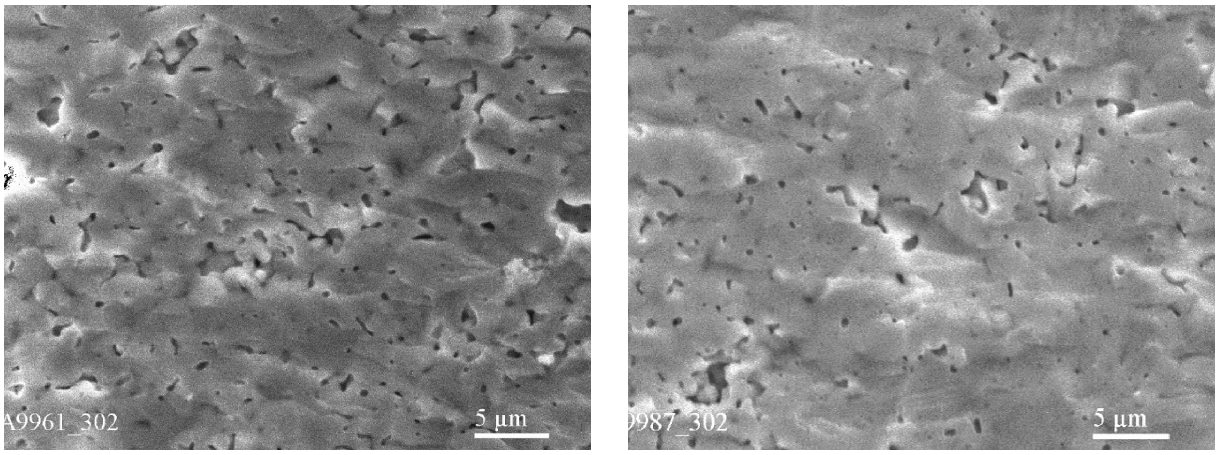

a *b*

Fig. 11. SEM fracture images of the 1Ce10ScSZ-Ukr powder isostatically pressed and sintered at 1550 °C: (*a*) 20 MPa and (*b*) 80 MPa

cleavage. The grain boundaries that can be considered as effective barriers to cleavage cracks are practically invisible. The fracture toughness of the isostatically pressed 1Ce10ScSZ-Ukr was 1.2–1.7 MPa·m$^{1/2}$, the highest among the three studied samples.

The grain growth in 1Ce10ScSZ ceramics with temperature (Fig. 8*b*) demonstrated that all three 1Ce10ScSZ samples differ by their grain growth. The highest grain growth in the range of 0.25 μm and 4.0 μm was observed for 1Ce10ScSZ-Praxair. The 1Ce10ScSZ-DKKK sample had the grain size in the range of 2.5–3.5 μm, whereas 1Ce10ScSZ-Ukr sintered at 1550 °C for 1.5 h was more stable, which corresponded to the grain size growth in the range of 0.8–1.8 μm though it was very porous.

Based on the comparison of the fracture surfaces of isostatically and uniaxially pressed samples shown above it is possible to assume that the porosity is not the only one reason for the slow grain growth in 1Ce10ScSZUkr samples. Indeed, Fig. 11 gives the evidence that the grain size in rather dense isostatically pressed 1Ce10ScSZ-Ukr samples sintered at 1550 °C is obviously less than 5 μm at both pressures. The 1Ce10ScSZ-DKKK samples sintered at 1550 °C demonstrated that their grain size has been changed from 3–7 μm at 20 MPa to 7–25 μm at 80 MPa (Fig. 10 insets *a, b*). It seems that the reasons for so different grain growth behavior of 1Ce10ScSZ samples can be influenced by both the nature of agglomerates and the distribution of impurities along the agglomerates and the grain boundaries.

Electrical conductivity

Fig. 12 presents the Arrhenius plot of total electrical conductivity, measured at the temperature ranges of 350–727 °C in air. The maximum conductivity value in this range is 0.036 Scm^{-1} at 727 °C. The total electrical conductivity of our sample is higher than the one measured for the commercial DKKK powder on the whole range of temperatures but slightly lower than the data reported in reference 7, probably due to different processing conditions for the sample. At higher temperatures, the conductivity values for our material overpasses the other samples. The activation energy is 1.02 eV up to 727 °C, decreasing to 0.73 eV above this temperature. The total conductivity (bulk and grain boundary) at 700 °C

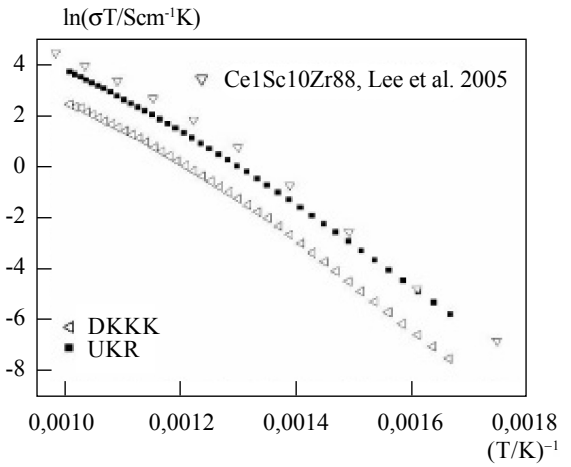

Fig. 12. The total conductivity (bulk and grain boundary) vs. temperature for the 1Ce10ScSZelectrolytes: ■ – Ukr, ◁ – DKKK, △ – Lee [7]

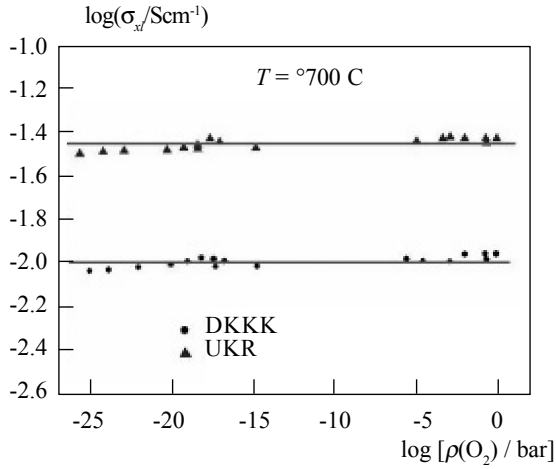

Fig. 13. The total conductivity (bulk and grain boundary) of the 1Ce10ScSZ electrolytes as a function of partial pressure of oxygen p(O_2) at 700 °C: ▲– Ukr, ● – DKKK

as a function of partial pressure of oxygen log p(O_2) is represented in Fig. 13 also showing that the conductivity of 1Ce10ScSZ-Ukr powder is higher than 1Ce10ScSZ-DKKK. It is possible to assume that the overall conductivity could be increased further by improving the sintering properties of 1Ce10ScSZ-Ukr powder. Fig. 14 depicts the long term testing in air, for 1500 hours at 800 °C, showing an initial decrease in conductivity for our sample of about 25% within 300 h followed by a constant evolution in time; in contrast, the conductivity of the commercial sample is almost constant for the

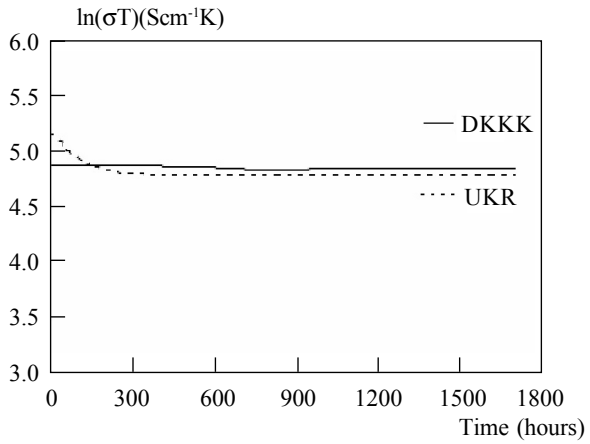

Fig. 14. Comparison of long term stability for our sample and the commercial one in air, at 800 °C (--- 1Ce10ScSZ Ukr and — DKKK)

time measured. Even like that, after 300 h the conductivities of the two samples are almost similar.

Conclusions

1. The comparative study of 1Ce10ScSZ-Ukr nano-powder produced from Ukrainian zircon-sands with its commercial counterparts 1Ce10ScSZ-DKKK, Japan, and Praxair, USA, was performed regarding their morphological, chemical, mechanical, and electrical properties.

2. It is shown that the size of initial particles in the Ukrainian powder is 20–50 nm; DKKK's is 100–200 nm, and Praxair's one is 100–300 nm. The specific surface area of powders is 48.28 m^2/g in Ukrainian, 11.61 m^2/g – in DKKK's; and 4.98 m^2/g – in Praxair's ones. DKKK's powder is practically non-agglomerated; Ukrainian one is assembled into rather soft agglomerates of average 2.4 μm size; and agglomerates of Praxair's powder is crystalline and rigid, practically closed for processing, of 18 μm size.

3. The results of the chemical analysis indicate that the concentration of the impurities in the bulk of the 1Ce10ScSZ-DKKK is only 0.001 wt.%, which is an order of magnitude lower than the corresponding values for 1Ce10ScSZ-Ukr and Praxair (0.01 wt.%). Regarding the nature of the contaminants, the 1Ce10ScSZ-Ukr is contaminated mainly with silica (0.05%) and alumina (<0.025%) while in 1Ce10ScSZ-Praxair mainly silica (0.05%) and titania (<0.14%) are present. Additional minor contamination in the form of K, Na, Ca, and Fe was also found in both powders. From the point of surface-bulk distribution, in 1Ce10ScSZ-DKKK, the surface of particles is enriched with Sc and Al; in 1Ce10ScSZ-Praxair, Sc and Si are mostly present on the surface. In 1Ce10ScSZ-Ukr, the surface is depleted with Sc; while Si is mostly localized in the bulk of the particles.

4. Uniaxially pressed 1Ce10ScSZ-Ukr samples demonstrated less sensitivity to the grain growth at high temperatures than 1Ce10ScSZ-Praxair and DKKK where the grain growth from 0.5 to 10 μm was detected after 1.5 h sintering at 1550 °C. Both 1Ce10ScSZ-Ukr powder and 1Ce10ScSZ-Praxair samples were insensitive to the isostatic pressure. On the contrary, in the case of 1Ce10ScSZ-DKKK the changes in isostatic pressure from 20 to 80 MPa resulted in the grain growth from 3–7 μm to 20–30 μm and the final significant decrease of the bending strength below 50 MPa.

5. Isostatically pressed and sintered at 1550 °C for 1.5 h 1Ce10ScSZ-Ukr samples had the density of 5.55 g/cm^3, bending strength of 100–120 MPa and 1.2–1.7 $MPa \cdot m^{1/2}$ fracture toughness. In comparison, the bending strength of 1Ce10ScSZ-Praxair samples at 5.55 g/cm^3 was similar with a value of about 100 MPa, however almost zero fracture toughness was detected. Finally, 1Ce10ScSZ-DKKK had 50–100 MPa bending strength and 0.7–1.2 $MPa \cdot m^{1/2}$ fracture toughness at 5.60 g/cm^3 density. The 1Ce10ScSZ-Ukr ceramics fail with cleavage; on the contrary, brittle intergranular and mixed mode cleavage and brittle intergranular mechanism was detected for 1Ce10ScSZ-DKKK and 1Ce10ScSZ-Praxair respectively.

6. The fracture mechanism of 1Ce10ScSZ-Ukr ceramics did not demonstrate any dependence on isostatic pressure. The highest biaxial strength was obtained for 1Ce10ScSZ-DKKK (375 MPa) sintered at 1350 °C. The second highest value was obtained for 1Ce10ScSZ-Ukr samples (250 MPa) sintered at 1500 °C. The lowest biaxial strength was detected for 1Ce10ScSZ-Praxair (220 MPa) sintered at 1450 °C.

7. Sintered at 1500 °C and higher the 1Ce10ScSZ-Ukr and Praxair samples demonstrated the same biaxial strength around 250 MPa while the value of biaxial strength for 1Ce10ScSZ-DKKK was only 150 MPa. The cleavage fracture mechanism was detected for 1Ce10ScSZ-Ukr samples without any changes with sintering temperature.

8. The electrical conductivity measurements at 250–800 °C indicated that the 1Ce10ScSZ-Ukr conductivity is higher than the conductivity of the commercially available 1Ce10ScSZ-DKKK samples. On long term testing, although our sample exhibits a continuous decrease of the conductivity value in the first 300 h, the attained value remain constant for the rest of the period and is almost displayed by the commercial sample. These conductivity values can be further improved by optimizing the sintering conditions for 1Ce10ScSZ-Ukr that already demonstrated a promising alternative to the commercial SOFC electrolyte materials.

The financial support from NATO «Science for Peace» Program, project number 980878 «Solid oxide fuel cells for energy security», is gratefully acknowledged. The authors would like to thank Dr. M. Bega and Dr. A. Kotko at Frantcevych Institute for Problems of Materials Science for their XRD and TEM studies and fruitful discussions, and Dr. V. Ivanov at Boreskov Institute of Catalysis for his SIMS studies.

Вивчено й порівняно властивості нанопорошків двоокису цирконію, стабілізованого двоокисами церію та скандію 1Ce10ScSZ, які виготовлено в Україні на Вільногірському державному гірничо-металургійному комбінаті (ВДГМК), в Японії компанією «Daiichi Kigenso Kagaku Kogyo» (DKKK) та в США компанією «Praxair». Порівняно з порошками виробництва DKKK та «Praxair» порошок виробництва ВДГМК (позначено як «Ukr») має найменший розмір частинок в інтервалі 20–50 нм. Міцність зразків, виготовлених із порошку «Ukr» із використанням ізостатичного пресування, становить 100–120 МПа при згині та є подібною до міцності порошку виробництва «Praxair». Міцність зразків виробництва DKKK менша (50–100 МПа) й залежить від ізостатичного тиску. Міцність одновісно пресованих зразків найвища в порошку DKKK (375 МПа), у зразках «Ukr» і «Praxair» вона становить відповідно 250 МПа та 220 МПа. Із-поміж трьох досліджених серій зразків найвищу електричну провідність при 700 °С мали електроліти, виготовлені з порошку «Ukr».

Ключові слова: *нанопорошки, стабілізований скандієм діоксид цирконію, 1Ce10ScSZ, твердий електроліт, тріщиностійкість, двовісна міцність, твердооксидні паливні елементи*

Были изучены и сравнены свойства нанопорошков двуокиси циркония, стабилизированного окислами церия и скандия 1Ce10ScSZ, которые произведены в Украине на Вольногорском государственном горно-металлургическом комбинате (ВГГМК), в Японии компанией «Daiichi Kigenso Kagaku Kogyo» (DKKK) и в США компанией «Praxair». В сравнении с порошками производства DKKK и «Praxair» у порошка производства ВГГМК (обозначен как «Ukr») наименьший размер частиц в интервале 20–50 нм. Прочность образцов, изготовленных из порошка «Ukr» с использованием изостатического прессования, составляет 100–120 МПа при изгибе и подобна прочности образцов из порошка производства «Praxair». Прочность образцов из порошка DKKK меньше (50–100 МПа) и зависит от давления изостатического прессования. Прочность одноосно прессованных образцов наиболее высока (375 МПа) у порошка DKKK, в образцах «Ukr» и «Praxair» она составляет соответственно 250 МПа и 220 МПа. Из трех испытанных серий образцов самая высокая электропроводность при 700 °С была у электролитов, изготовленных из порошка «Ukr».

Ключевые слова: *нанопорошки, стабилизированный скандием диоксид циркония, 1Ce10ScSZ, твердый электролит, трещиностойкость, двухосная прочность, твердооксидные топливные элементы*

1. *Aroutiounian V.* Metal oxide hydrogen, oxygen, and carbon monoxide sensors for hydrogen setups and cells // Int. Journal of Hydrogen Energy. – 2007. – N 32. C. 1145–1158.
2. *Verda V., Quaglia M.C.* Solid Oxide Fuel Cells for distributed power generation and co-generation // Int. Journal of Hydrogen Energy. – 2008. – N 33. – C. 2087–2096.
3. *Progress* in high-temperature electrolysis for hydrogen production using planar SOFC technology / Herring J.S., O'Brien J.E., Stoots C.M. et al. // Int. Journal of Hydrogen Energy. – 2007. – N 32. – C. 440–450.
4. *Nonstoichiometry* and electrical transport in Sc-doped zirconia / Kosacki I., Anderson H.U., Mizutani Y. et al. // Solid State Ionics. – 2002. – N 152–153. – C. 431–438.
5. *Solid* oxide fuel cell (SOFC) using industrial grade mixed rare-earth oxide electrolytes / Zhu B., Liu X., Zhu Z. et al. // Int. Journal of Hydrogen Energy. – 2008. – N 33. – C. 3385–3392.
6. *Degradation* of the electrical conductivity in stabilized zirconia system. Part II: Scandia-stabilized zirconia / Haering C., Roosen A., Schichl H. et al. // Solid State Ionics. – 2005. – N 176. – C. 261–268.
7. *Characterization* of ZrO_2 co-doped with Sc_2O_3 and CeO_2 electrolyte for the application of intermediate temperature SOFCs / Lee Д-S., Kim W.S., Choi S.H. et al. // Solid State Ionics. – 2005. – N 176. – C. 33–39.

8. *Appel C., Bonanos N.* Structural and electrical characterization of silica-containing yttria-stabilized zirconia // J. European Ceramic Society. – 1999. – **19**, N 6–7. – C. 847–851.
9. *Zirconia* powders stabilized with Scandia and their ceramics: Part 1. Mechanical behavior / Vasylyev O., Koval O., Brychevskyi M. et al. // In Proc. Conf. «Fuel Cells and Energy Storage Systems: Materials, Processing, Manufacturing and Power Management Technologies», Materials Science & Technology 2006 Conference and Exhibition (MS&T'06), October 15–19, 2006, Cincinnati, USA, Ed. P. Singh et al. – Vol. 1. – P. 315–326.
10. *Vereschak V.G., Nikolenko N.V., Nosov K.V.* Nanocristalline powders system ZrO_2-Sc_2O_3 for solid-state combustion cells // Fuel Cell Technologies: State and Perspectives, NATO Science Series. II. Mathematics, Physics and Chemistry. – Vol. 202. – P. 317–321.
11. *Vaija J., Lagaude A., Ghommidh C.* Evaluation of image analysis and laser granulometry for microbial cell sizing // Biomedical and Life Sciences. – 1993. – N 45. – C. 483–487.
12. *Creep* in Scandia stabilized Zirconia / Kilo M., Argirusis C., Borchardt G. et al. // Solid State Ionics. – 2008. – **179**, N 21–26. – C. 804-806.